





Article

A Linear Quadratic Integral Controller for PV-Module Voltage Regulation for the Purpose of Enhancing the Classical Incremental Conductance Algorithm

Noureddine Bouarroudj ¹, Yehya Houam ¹, Abdelhamid Djari ², Vicente Feliu-Batlle ^{3,*},
Abdelkader Lakhdari ¹ and Boualam Benlahbib ¹

¹ Unité de Recherche Appliquée en Energies Renouvelables, URAER, Centre de Développement des Energies Renouvelables, CDER, Ghardaïa 47133, Algeria; autonour@gmail.com (N.B.); yahiahouam@gmail.com (Y.H.); lakhdari_abdelkader@hotmail.com (A.L.); bouallam30@gmail.com (B.B.)

² Electrical Engineering Department, Echahid Cheikh Larbi Tebessi, University-Tebessa, Tebessa 12022, Algeria; abdelhamid.djari@univ-tebessa.dz

³ School of Industrial Engineering and Instituto de Investigaciones Energéticas y Aplicaciones Industriales, University of Castilla-La Mancha, Av. Camilo Jose Cela, S/N, C.P. 13001 Ciudad Real, Spain

* Correspondence: vicente.feliu@uclm.es

Abstract: As a result of the exhaustion of fossil energy sources and the corresponding increase of their negative environmental impact, recent research has intensively focused on regions of alternative energy resources and, especially, on solar energy. Slow tracking of the maximum power point (MPP) and fluctuations around the MPP reduce the efficiency of photovoltaic power generation systems (PV). This study offers a novel design for the MPPT controller, which we refer to as the “hybrid IC-LQI approach”, which combines the incremental conductance (IC) technique and the linear quadratic integral (LQI) controller based on the boost converter’s small signal model. We conduct a comparative study of the proposed hybrid IC-LQI, and the classical one-stage IC technique in order to show the effectiveness of our proposal under three different scenarios of weather conditions and load. According to simulation findings, the proposed hybrid IC-LQI approach has a high tracking efficiency of up to 98.92%, owing to faster tracking of MPP with very large reduction of oscillations. On the other hand, the IC technique provides less efficiency, up to 96.1%, showing very slow tracking and high oscillations. The presented analysis of the results confirms the superior performance of the developed hybrid IC-LQI technique to the classical IC technique.

Keywords: PV-system; MPPT; IC-algorithm; IC-LQI algorithm



Citation: Bouarroudj, N.; Houam, Y.; Djari, A.; Feliu-Batlle, V.; Lakhdari, A.; Benlahbib, B. A Linear Quadratic Integral Controller for PV-Module Voltage Regulation for the Purpose of Enhancing the Classical Incremental Conductance Algorithm. *Energies* **2023**, *16*, 4532. <https://doi.org/10.3390/en16114532>

Academic Editor: Anastasios

Dounis

Received: 3 May 2023

Revised: 24 May 2023

Accepted: 1 June 2023

Published: 5 June 2023



Copyright: © 2023 by the authors. Licensee MDPI, Basel, Switzerland. This article is an open access article distributed under the terms and conditions of the Creative Commons Attribution (CC BY) license (<https://creativecommons.org/licenses/by/4.0/>).

1. Introduction

Recent research shows that, in recent years, the global demand of photovoltaic energy in power generation systems is growing very fast. Moreover, the recent evolution of the equipment of PV energy systems and their usage-related factors, such as the increase of PV cell effectiveness, the decrease of the manufacturing and installation costs, and the enhanced structural insertion to buildings, have increased the demand for these systems [1]. However, the low efficiency of the power conversion of MPPT controllers in PV power production systems remains as one of the biggest barriers to operate these systems at the maximum extracted power point, which is a very important problem that is worth studying. Indeed, improving the yield of MPPT controllers automatically implies a great improvement of the overall system yield [2]. In this context, it should be noted the negative impact of the variation of weather conditions-like solar irradiation and ambient temperature-in the efficiency of the MPPT controller [3]. Since the change of weather conditions is a persistent problem throughout the year, the tracking of the MPP of the PV-systems is a difficult problem that has been approached using several techniques.

Two of the most used algorithms are the one stage perturbation and observation (P&O) [4] and the incremental conductance (IC) [5], due to their simple realization and implementation with low cost. One degree of freedom direct control distinguishes these two algorithms from one another. The duty cycle step size, which directly influences the output power of the PV module, represents the degree of freedom. Selecting a too big step size produces power loss because large power fluctuations appear around the MPP; and selecting a too small step size produces very slow PV-module power responses [6]. Next, we mention some articles that try to solve these drawbacks.

Some guidelines about the perturbation frequency and its relationship with the step size were provided in [6], which stabilized the MPP in steady state without oscillations in a variable climatic condition. A variable step size P&O [7] and a variable step size IC algorithm [8,9] have also been proposed. These two approaches consider the behavior of the PV-system to compute the step size in an adaptive way, which changes based on the separation between the MPP zone and the PV-system operating point. Despite the good results provided by these improved methods in terms of speed of response, stability and smooth steady-state PV-module power under changing climatic conditions, they have limitations and inability to track the global MPP when a PV panel is just partially shaded [10].

Another solution to surpass the disadvantages of the classical P&O and IC methods is the use of two stages of control. In this case, the strategy becomes more flexible since there is more than one degree of freedom. An integrator controller tuned by the Routh stability criterion and based on a linear small signal model was proposed in [11–13] to enhance the IC algorithm. Through this technique, the user can find the value of the integrator constant in terms of the load value, no matter how it changes, to preserve the stability of the voltage-closed loop. The results of applying this approach show its superiority to the classical IC algorithm in term of stability in the steady state, smooth PV-module output power and efficiency. To cope with the variable states, uncertainties and disturbances, which can affect directly and negatively the PV-system performance, [14] proposed a terminal sliding mode approach.

The findings of a simulation and an experiment show the superiority of the IC sliding mode approach to the IC proportional integral (PI) controller in low and high irradiance tests. In the same direction, [15] proposed a combination of the (P&O) and the sliding mode approach with a PID sliding surface, including an adaptation law to alter the controller parameters in different weather conditions. Comparative studies using simulation and practical implementation show the dominance of this approach over the classical P&O with direct control and the P&O-PI algorithms. To tackle the imperfections (chattering phenomenon and steady state error) of the classical sliding mode control of MPPT, a hybrid approach was proposed in [16] that combined integral backstepping and sliding mode control. Practical results shown the high dynamic performance of this approach against the conventional sliding mode control. To surpass the drawback of the classical PID controller (in the second stage of MPPT controller) of having to retune its gains when the system parameters change, an adaptive neural network based on radial basis functions [17] was proposed which proved to be superior to classical algorithms.

Most of the above mentioned MPPT techniques give satisfactory results but they do not provide an optimal performance since the determination of the parameters of the controllers are not based on the optimization of any cost function. In this paper we suggest combining an IC algorithm (because of its high efficiency and superiority over P&O [18]) with a linear quadratic integral controller, which will be detailed in the rest of the paper.

2. Stand-Alone Photovoltaic System Description and Modeling

A photovoltaic system is a set of elements for producing electricity, using a solar source. These constituents are essentially the PV-panel, the DC-DC converter controlled by an MPPT controller, and the load (see Figure 1). In the majority of cases, a stand-alone PV system requires batteries or other storage devices for its use during periods of

solar unavailability (Ex: night-time, non-sunny periods) [19]. This paper only focuses on developing an MPPT controller for the maximum power harvesting from the PV-module. In the following subsection, the details of each element of this system are given.

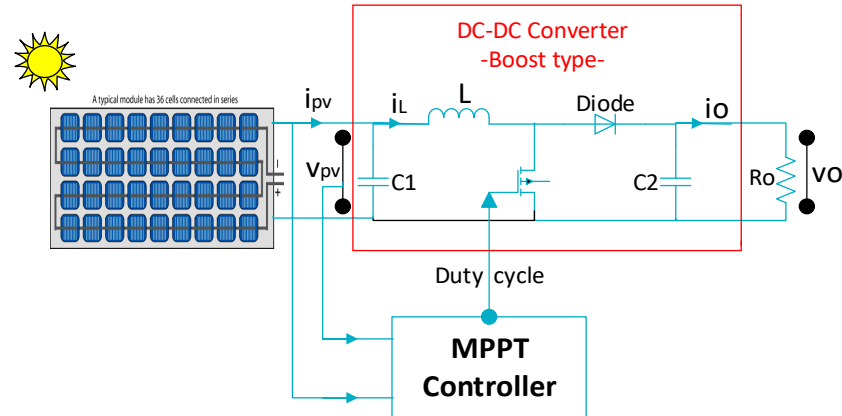


Figure 1. Synoptic scheme of a PV-system equipped with an MPPT controller algorithm.

2.1. PV-Module Modeling and Electrical Properties

To obtain the appropriate voltage and current levels, numerous photovoltaic cells are connected in series and parallel to form a PV-module. Essentially, a PV cell is a P-N semiconductor junction. There is a direct current produced when exposed to light. To simplify, electrical models with a single diode or multi diodes [20] are generally used. In this paper, a typical two-diodes electrical model of a PV-cell is used, which is represented in Figure 2. A photocurrent (I_{ph}), two diodes, a parallel resistance (R_p) that symbolizes a leakage current, and a series resistance (R_s) caused by the interaction of semiconductors with metal components make up the analogous circuit of the general model, as shown in this figure.

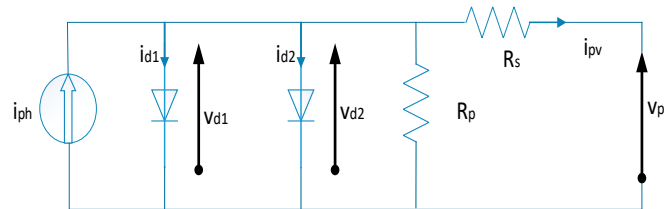


Figure 2. Typical electrical model with two diodes of a PV-cell.

In accordance with the electrical model in Figure 2, the following is the PV-module mathematical model:

$$N_p \cdot i_{pv} = i_{ph} - i_{sat1} \cdot \left(\exp\left(\frac{q \cdot (v_{pv} + i_{pv} \cdot N_s \cdot R_s)}{N_s \cdot n_1 \cdot k \cdot T}\right) - 1 \right) - i_{sat2} \cdot \left(\exp\left(\frac{q \cdot (v_{pv} + i_{pv} \cdot N_s \cdot R_s)}{N_s \cdot n_2 \cdot k \cdot T}\right) - 1 \right) - \frac{v_{pv} + i_{pv} \cdot N_s \cdot R_s}{N_s \cdot R_p} \quad (1)$$

where:

- $i_{ph} = S \cdot i_{sc}$: photo-generated current (A). S is the irradiance.
- i_{sat1}, i_{sat2} : diode saturation currents (A). Their mathematical formulas and parameters are detailed in [17].
- n_1, n_2 : ideality factors of the diodes
- N_s : number of PV-cells connected in series
- N_p : number of PV-cells connected in parallel
- k : constant of Boltzmann ($1.3806503 \times 10^{-23}$ J/K)
- T : temperature (K)
- q : charge of electron ($1.60217646 \times 10^{-19}$ Coulombs)

Table 1 shows the physical and electrical characteristics of the used PV-module.

Table 1. Electrical characteristics for the used PV-module.

Maximum PV-module power (P_{max})	≈ 61.92 W
Open circuit PV-module voltage (v_{oc})	25.25 V
PV-module short circuit current (i_{sc})	3.25 A
PV-module voltage at maximum power (v_{mpp})	20 V
PV-module current at maximum power (i_{mpp})	≈ 3.1 A
factor of ideality n_1	1
factor of ideality n_2	2
Number of PV-cells connected in series (N_s)	36
Number of PV-cells connected in parallel (N_p)	1

A Matlab/Simulink program is used to implement the PV-module model. The operation of this model is simulated over a range of irradiance and temperature conditions. Then the effect of each parameter on the performance of our PV-module is studied. The simulation results are given in Figure 3.

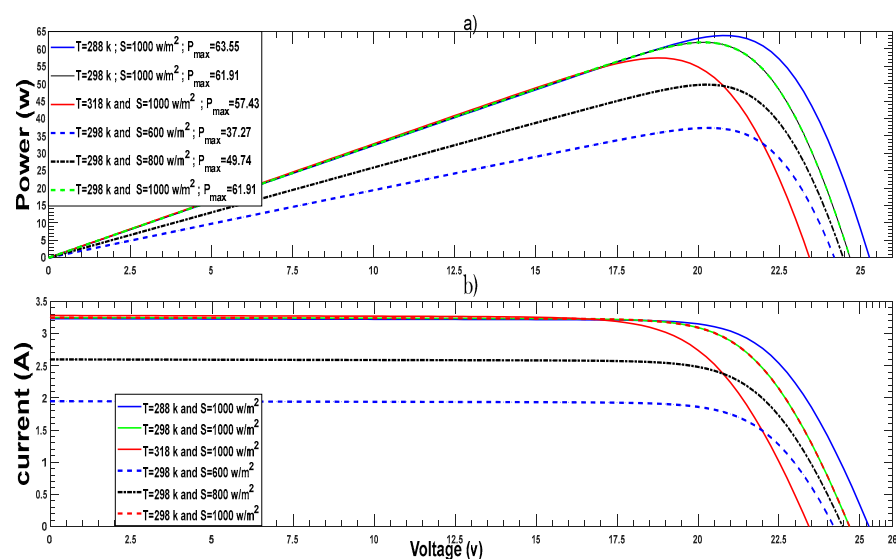


Figure 3. (a) power-voltage and (b) current-voltage characteristics of the used PV module for different irradiance and temperature levels.

According to the above curves, we notice that the irradiation has a very remarkable impact on the power and current. In particular, the current increases with the growth of the irradiance. Thus, we can conclude that the efficiency of a PV module increases considerably with the increase in irradiance S .

The above curves show that the open circuit voltage v_{oc} decreases as the temperature increases. Then a high temperature has a negative impact on the performance of a PV module.

It is worth to note that there are some other factors that can affect the efficiency of the PV-module like the ideality factors of diodes, series and parallel resistors . . . etc. These will be considered constant in this work. Additionally, we deal with this PV module as an energy source only, and the MPPT algorithm detailed below is valid for any other model of photovoltaic panel.

2.2. Modeling of DC-DC Boost Converter

Figure 3 shows how the variation in temperature and irradiance have a significant impact on the maximum output power of the PV-module. For these reasons, a controller for tracking the maximum power point is indispensable. The DC-DC boost converter of Figure 1 is used to implement the MPPT controller. It is controlled by a duty cycle α of a PWM signal, which yields the following relationships between the input and output voltages, and the input and output currents:

$$\begin{cases} \frac{v_o}{v_{pv}} = \frac{1}{(1-\alpha)} \\ \frac{i_o}{i_{pv}} = (1-\alpha) \end{cases} \tag{2}$$

Combining the two sub-models obtained when the switch position is ON or OFF, the following equations are determined to describe the approximate model of the boost converter [21] with a resistive load R_o :

$$\begin{cases} \frac{dv_{pv}}{dt} = \frac{(i_{pv}-i_L)}{C_1} \\ \frac{di_L}{dt} = \frac{v_{pv}-(1-\alpha)\cdot v_o}{L} \\ \frac{dv_o}{dt} = \frac{(1-\alpha)\cdot i_L - (\frac{v_o}{R_o})}{C_2} \end{cases} \tag{3}$$

The values of the various boost converter components are set as in [12]: $L = 0.5$ mH, $C_1 = 1000$ μ F, $C_2 = 470$ μ F.

Our proposal of MPPT requires the linearization of the non-linear model (3). This linearization can be carried out in several ways, but the most used is the small signal modeling method. By “small signals” we mean low amplitude signals that are deviations from the DC values. In this approach, the state variables v_{pv} , i_L , v_o , α can be rewritten, respectively, as: $v_{pv} = v_{pv(opt)} + \hat{v}_{pv}$, $i_L = i_{L(opt)} + \hat{i}_L$, $v_o = v_{o(opt)} + \hat{v}_o$, $\alpha = \alpha_{opt} + \hat{\alpha}$, where \hat{v}_{pv} , \hat{i}_L , \hat{v}_o , $\hat{\alpha}$ are low amplitude signals. Components $v_{pv(opt)}$, $i_{L(opt)}$, $v_{o(opt)}$, and α_{opt} are DC values calculated in standard temperature and lossless boost converter conditions [12]. By neglecting the two small quantities $\frac{\hat{\alpha}\cdot\hat{v}_o}{L}$ and $\frac{\hat{\alpha}\cdot\hat{i}_L}{C_2}$ the boost converter model for small signals becomes:

$$\begin{cases} \frac{d\hat{v}_{pv}}{dt} = \frac{(\hat{i}_{pv}-\hat{i}_L)}{C_1} \\ \frac{d\hat{i}_L}{dt} = \frac{\hat{v}_{pv}-(1-\alpha_{opt})\cdot\hat{v}_o+\hat{\alpha}\cdot v_{o(opt)}}{L} \\ \frac{d\hat{v}_o}{dt} = \frac{(1-\alpha_{opt})\cdot\hat{i}_L - (\frac{\hat{v}_o}{R_o}) - \hat{\alpha}\cdot i_{L(opt)}}{C_2} \end{cases} \tag{4}$$

Taking into account that the relation between \hat{i}_{pv} and \hat{v}_{pv} is $\hat{i}_{pv} = \frac{-1}{R_{mpp}}\cdot\hat{v}_{pv}$ [22] and the relation between R_{mpp} and the load gain R_o is $R_{mpp} = R_o\cdot(1-\alpha_{opt})^2$ [12], the small signal state-space model of the interfacing boost converter is

$$\begin{cases} \dot{x} = A\cdot x + B\cdot\hat{\alpha} \\ y = C\cdot x + D\cdot\hat{\alpha} \end{cases} \tag{5}$$

where

$$A = \begin{bmatrix} \frac{-1}{C_1\cdot R_o\cdot(1-\alpha_{opt})^2} & \frac{-1}{C_1} & 0 \\ \frac{1}{L} & 0 & \frac{-(1-\alpha_{opt})}{L} \\ 0 & \frac{1-\alpha_{opt}}{C_2} & \frac{-1}{C_2\cdot R_o} \end{bmatrix}$$

$$B = \begin{bmatrix} 0 \\ \frac{v_{o(opt)}}{L} \\ \frac{-i_{L(opt)}}{C_2} \end{bmatrix}$$

$$C = [1 \quad 0 \quad 0]$$

$$D = 0$$

$x = [\hat{v}_{pv} \quad \hat{i}_L \quad \hat{v}_o]^T$ is the state vector and y is the output vector.

3. Implementation of MPPT Algorithms

In the following subsections, details of the studied MPPT methods are given. First, the classical fixed step size duty cycle IC algorithm is presented, and its drawbacks are mentioned. Second, an MPPT method that combine fixed voltage step size IC algorithm with a linear controller is presented to overcome the disadvantages of the first MPPT controller.

3.1. One Stage Classical IC Algorithm

The maximum power point (MPP) can only be reached if dp_{pv}/dv_{pv} is zero, which is the foundation of the IC method [23]. Knowing that $p_{pv} = i_{pv} \cdot v_{pv}$, the product's derivative with regard to voltage v_{pv} yields the following relationship:

$$\frac{dp_{pv}}{dv_{pv}} = \frac{d(v_{pv} \cdot i_{pv})}{dv_{pv}} = i_{pv} + v_{pv} \cdot \frac{di_{pv}}{dv_{pv}} \quad (6)$$

At MPP, since dp_{pv}/dv_{pv} is zero, the following equality is verified:

$$\frac{di_{pv}}{dv_{pv}} = -\frac{i_{pv}}{v_{pv}} \quad (7)$$

When the operating point is at the left of the MPP we have that:

$$\frac{i_{pv}}{v_{pv}} > -\frac{di_{pv}}{dv_{pv}} \quad (8)$$

and when the operating point is at the right of the MPP: $\frac{i_{pv}}{v_{pv}} + \frac{di_{pv}}{dv_{pv}} < 0$

$$\frac{i_{pv}}{v_{pv}} < -\frac{di_{pv}}{dv_{pv}} \quad (9)$$

Figure 4 shows a flowchart of the commonly used IC algorithm. The current and previous values of the voltage and current of the PV-module are used to calculate the values of di_{pv} and dv_{pv} . If $dv_{pv} = 0$ and $di_{pv} = 0$, then the atmospheric conditions have not changed, and the system is still operating at the MPP. If $di_{pv} > 0$ and $dv_{pv} = 0$, then the amount of solar irradiance has increased, raising the voltage from the maximum power point. This requires the system to decrease the duty cycle of the boost converter to locate a new point of maximum power. Conversely, if $di_{pv} < 0$, the amount of solar irradiance has decreased, thus lowering the maximum power point voltage and requiring the system to increase the duty cycle. If the changes in voltage and current are not zero, the ratios of Equations (8) and (9) are used to govern the direction in which the duty cycle must change, in order to reach the maximum power point.

3.2. Hybrid MPPT Algorithm

Using a second stage of controllers in the IC method can make the amount $\frac{i_{pv}}{v_{pv}} + \frac{di_{pv}}{dv_{pv}}$ trend almost to the zero-target value and lessen the steady state error created by the MPPT controller when looking for the MPP because the amount $\frac{i_{pv}}{v_{pv}} + \frac{di_{pv}}{dv_{pv}}$ never approaches zero in a practical implementation. Additionally, compared to the conventional one stage IC method, it decreases the oscillation's amplitude once the MPP is reached and improves the PV system's efficacy and efficiency [12,24]. Figure 5 depicts this technique, with the first stage used to search for the reference/optimal voltage and the second stage used to control the DC-DC boost converter.

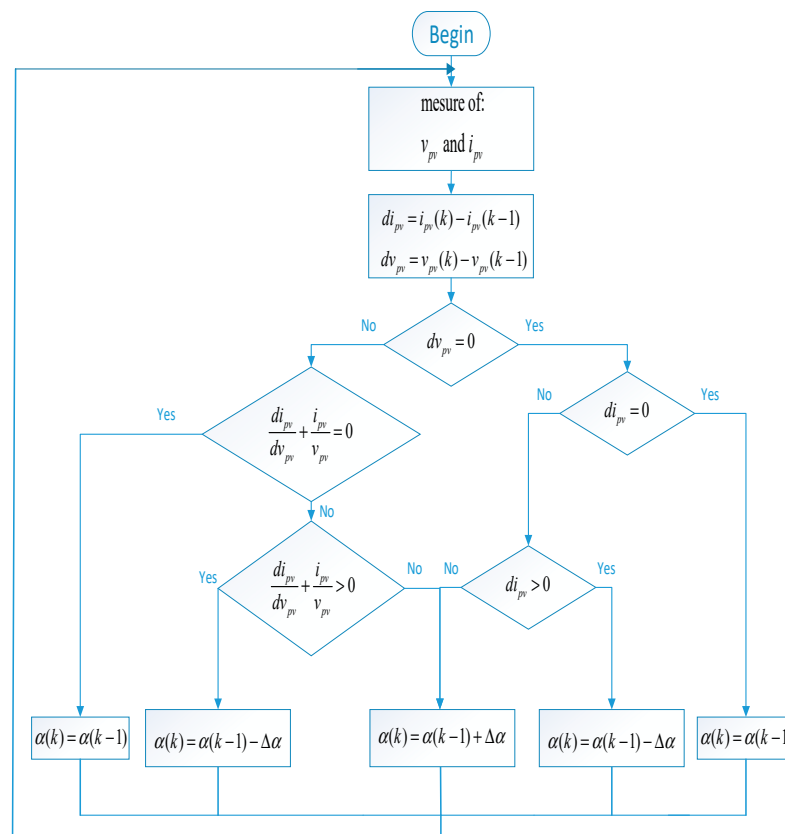


Figure 4. Flowchart of the commonly used one stage IC algorithm.

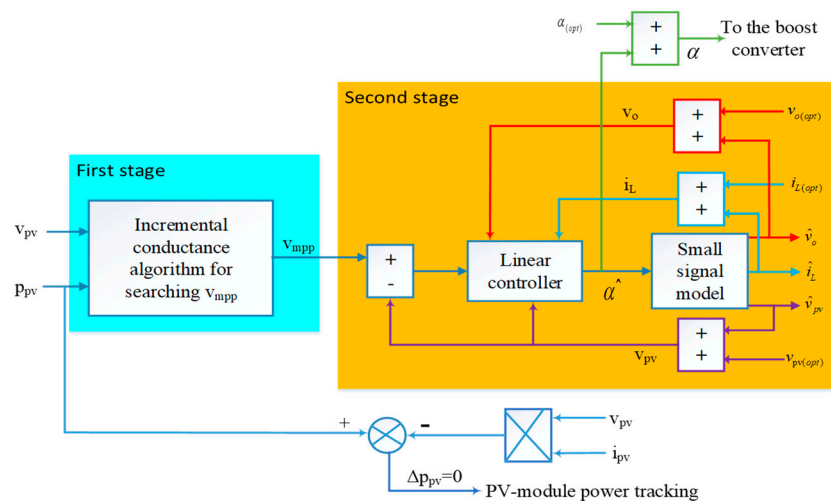


Figure 5. Scheme of hybrid IC algorithm and linear control.

The optimal voltage search is ensured using a mechanism similar to the one of Figure 4, but with the following restrictions:

- (a) when $\alpha(k) = \alpha(k - 1) - \Delta\alpha$, the $v_{mpp}(k)$ must be equal to $v_{mpp}(k - 1) + \Delta v$. This implies that the operating point of the PV-module is in the left half plane (see Figure 6). In order to reach the MPP, the voltage must be increased.
- (b) when $\alpha(k) = \alpha(k - 1) + \Delta\alpha$, the $v_{mpp}(k)$ must be equal to $v_{mpp}(k - 1) - \Delta v$. This implies that the operating point of the PV-module is in the right half plane (see Figure 6). In order to reach the MPP, the voltage must be reduced.

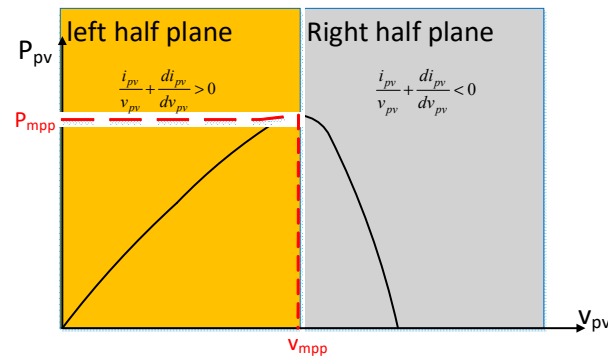


Figure 6. Right and left half planes in a $p_{pv} - v_{pv}$ curve defining the operation of the PV-system.

To ensure the optimal voltage (v_{mpp}) tracking with a null steady state error, a controller with an integral term must be used. LQI controller has been used because of its simplicity, robustness, and near-optimal performance.

Remark: The incremental conductance algorithm in the first stage cannot give the global MPP for the following reason: if we start with $\alpha = 0$ for $t = 0$, then the algorithm will fall directly into the first local MPP and this is when $\frac{i_{pv}}{v_{pv}} + \frac{di_{pv}}{dv_{pv}} = 0$.

Hybrid IC-LQI Algorithm

The LQR control is of the proportional type. To improve its performance in the presence of constant disturbances, and to achieve null steady state error to step commands, it is desirable to add an integral effect. This is denoted the LQI controller, and its mathematical formulation will be subsequently detailed.

a- State-space representation of error dynamics

The design of the LQI controller requires the addition of an extra state to the state space detailed previously. This augmented state-space representation is:

$$\dot{x}(t) = A \cdot x(t) + B \cdot \hat{\alpha}(t) \tag{10}$$

$$y(t) = C \cdot x(t) + D \cdot \hat{\alpha}(t) \tag{11}$$

$$\dot{e}(t) = v_{mpp}(t) - \hat{v}_{pv}(t) = v_{mpp}(t) - C \cdot x(t) \tag{12}$$

The duty cycle command of the state feedback for the augmented state-space system is given by:

$$\hat{\alpha}(t) = -K \cdot x(t) - k_i \cdot e(t) \tag{13}$$

where $K_{(1 \times 3)} = [k_1 \quad k_2 \quad k_3]$ is the gain matrix of the state feedback, and k_i is the integral gain.

The augmented state-space system that combines (10) and (12) is

$$\begin{bmatrix} \dot{x}(t) \\ \dot{e}(t) \end{bmatrix} = \begin{bmatrix} A & 0 \\ -C & 0 \end{bmatrix} \cdot \begin{bmatrix} x(t) \\ e(t) \end{bmatrix} + \begin{bmatrix} B \\ 0 \end{bmatrix} \cdot \hat{\alpha}(t) + \begin{bmatrix} 0 \\ I \end{bmatrix} \cdot v_{mpp}(t) \tag{14}$$

In steady state, Equation (14) can be rewritten as:

$$\begin{bmatrix} \dot{x}(\infty) \\ \dot{e}(\infty) \end{bmatrix} = \begin{bmatrix} A & 0 \\ -C & 0 \end{bmatrix} \cdot \begin{bmatrix} x(\infty) \\ e(\infty) \end{bmatrix} + \begin{bmatrix} B \\ 0 \end{bmatrix} \cdot \hat{\alpha}(\infty) + \begin{bmatrix} 0 \\ I \end{bmatrix} \cdot v_{mpp}(\infty) \tag{15}$$

Assuming that v_{mpp} is a constant input, subtracting (15) from (14) yields the new error dynamics:

$$\begin{bmatrix} \dot{x}_e(t) \\ \dot{e}_e(t) \end{bmatrix} = \begin{bmatrix} A & 0 \\ -C & 0 \end{bmatrix} \begin{bmatrix} x_e(t) \\ e_e(t) \end{bmatrix} + \begin{bmatrix} B \\ 0 \end{bmatrix} \cdot \hat{\alpha}_e(t) \quad (16)$$

where

$$x_e(t) = x(t) - x(\infty) \quad (17)$$

$$e_e(t) = e(t) - e(\infty) \quad (18)$$

$$\hat{\alpha}_e(t) = \hat{\alpha}(t) - \hat{\alpha}(\infty) \quad (19)$$

Let us define $\zeta(t) = \begin{bmatrix} x_e(t) \\ e_e(t) \end{bmatrix}$. Then Equation (19) can be rewritten as:

$$\dot{\zeta}(t) = \bar{A} \cdot \zeta(t) + \bar{B} \cdot \hat{\alpha}_e(t) \quad (20)$$

where $\bar{A} = \begin{bmatrix} A & 0 \\ -C & 0 \end{bmatrix}$ and $\bar{B} = \begin{bmatrix} B \\ 0 \end{bmatrix}$.

Combining (13) with (17)–(19), it is obtained that

$$\hat{\alpha}_e(t) = -\bar{K} \cdot \zeta(t) \quad (21)$$

where

$\bar{K} = [K \quad k_i]$ and combining (20) and (21) yields the closed-loop error dynamics:

$$\dot{\zeta}(t) = (\bar{A} - \bar{B} \cdot \bar{K}) \cdot \zeta(t) \quad (22)$$

which shows that the gain matrix \bar{K} has to be designed adequately to allow $\zeta(t)$ converge to zero.

b- LQI controller design

The LQI control is based on determining the gain matrix \bar{K} that makes error dynamics (20) stable [25]. The following quadratic cost function J is minimized to determine the gain matrix \bar{K} :

$$J = \int_0^{\infty} \left(x_e^T(t) \cdot Q \cdot x_e(t) + \hat{\alpha}_e^T(t) \cdot R \cdot \hat{\alpha}_e(t) \right) \cdot dt \quad (23)$$

where R and Q are weight matrices. These matrices are positive definite, and their elements are chosen to ensure a balance between the energy of the control signal α_e at the input of the system and the energy of the state variables x_e , which depends strongly on the response speed.

The following formula yields the optimal gain matrix \bar{K} that minimizes the criterion J :

$$\bar{K} = [-K \quad -k_i] = R^{-1} \cdot \bar{B} \cdot P \quad (24)$$

where P is a positive-definite matrix that represents the *Ricatti* equation's solution:

$$\bar{A} \cdot P + P \cdot \bar{A} - P \cdot \bar{B} \cdot R^{-1} \cdot \bar{B} \cdot P + Q = 0 \quad (25)$$

Combining (21) and (24) gives:

$$\hat{\alpha}_e(t) = -R^{-1} \cdot \bar{B} \cdot P \cdot \zeta(t) \quad (26)$$

and the optimal control law for the duty cycle of system (10) is:

$$\hat{\alpha}(t) = -R^{-1} \cdot \bar{B} \cdot P \cdot \begin{bmatrix} x(t) \\ e(t) \end{bmatrix} \quad (27)$$

The duty cycle with the optimal gain matrix will drive the voltage error $e(t)$ to zero and the system states (v_{pv} , i_L and v_o) toward their desired values in steady states. The scheme of the LQI controller proposed for the PV-module voltage is given in Figure 7.

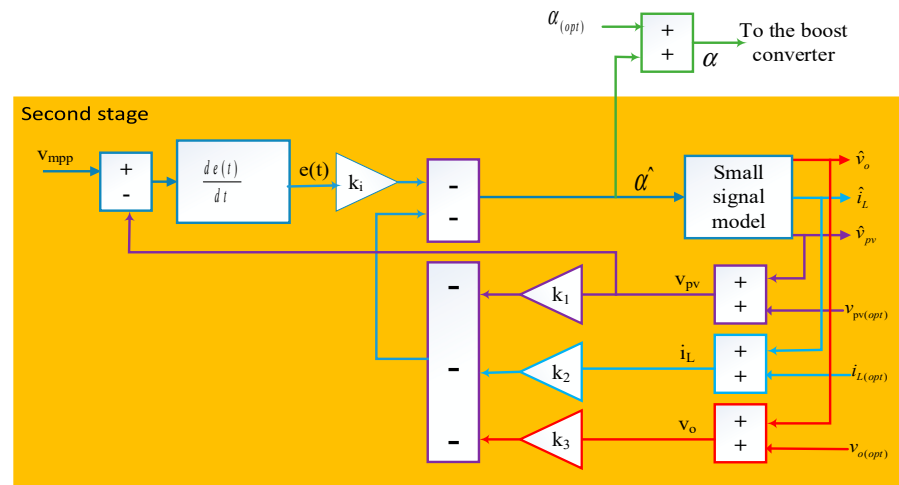


Figure 7. Scheme of proposed hybrid IC-LQI algorithm.

The most challenging aspect of designing an LQI controller is the proper choice of Q and R . Bryson's rule provides a logical, straightforward option for the matrices Q and R [26]. Although Bryson's rule typically produces positive outcomes, it is frequently just the beginning of an iterative design process that involves trial and error and aims to produce desirable attributes for the closed-loop system. Based on this rule, Q and R are matched, respectively, with the following values: $R = 1 \times 10^{-4}$ and $Q = \text{diag}([0,0,0,1])$, which gives the gains of the LQI controller: $k_i = 100$ and $K = [-0.0619 \quad 0.0320 \quad -0.0064]$.

Remarks: (1) In comparison to the classical IC algorithm, the synthesis of the hybrid IC-LQI MPPT controller requires the use of four sensors to measure the four states. The designer can make use of an observer to get around this problem.

(2) MPPT technique can be applied to single module configurations as well as larger PV arrays.

4. Simulation Results and Discussion

In this section, the proposed MPPT algorithms are implemented in a Matlab/Simulink program (as shown in Figure 8) with a sample time of 10^{-4} s and a voltage step size $\Delta v = 10^{-3}$ volt. The proposed hybrid IC-LQI algorithm is compared with the classical one-stage IC algorithm with different duty cycle step size. The simulation is carried out under different scenarios which are very common in real world, as detailed in the following subsections.

4.1. First Test Scenario: Simulation under Standard Test Condition (STC)

A 25°C cell temperature and a 1000 W/m^2 irradiance with an air mass 1.5 (AM1.5) spectrum are required by the STC, an industry standard used to describe the performance of PV modules. These are the irradiance and spectrum of sunlight incident on a sun-facing surface at a 37° tilt with the sun at an angle of 41.81° above the horizon on a clear day. Under these conditions, the MPP of the PV-module and the duty cycle using the synthesized MPPT controllers are given respectively in Figures 9 and 10. Figure 9 shows that the different MPPT methods provided the MPP but with different performances. The PV-system with the classical one-stage IC algorithm with $\delta\alpha = 10^{-4}$ requires long time to reach the MPP while choosing $\delta\alpha = 5 \times 10^{-4}$ yields a response too fast but with big steady state oscillations around the MPP. These drawbacks of the classical one-stage IC algorithm are suppressed using hybrid IC-LQI algorithm. The PV-module power response using this last algorithm is smooth, without oscillations, and faster compared to the classical one.

The command signals in Figure 10 that stable at 63.75% guarantee these outcomes. In this figure, the command signal provided by the proposed MPPT controller is the best one in term of rapidity and smoothness.

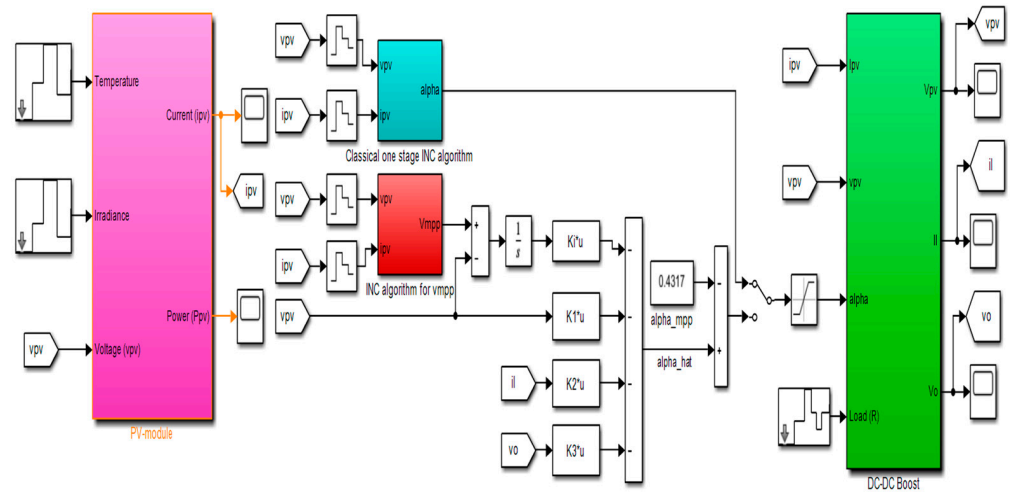


Figure 8. Proposed MPPT approach-based IC-LQI controller for PV-system using Matlab/Simulink.

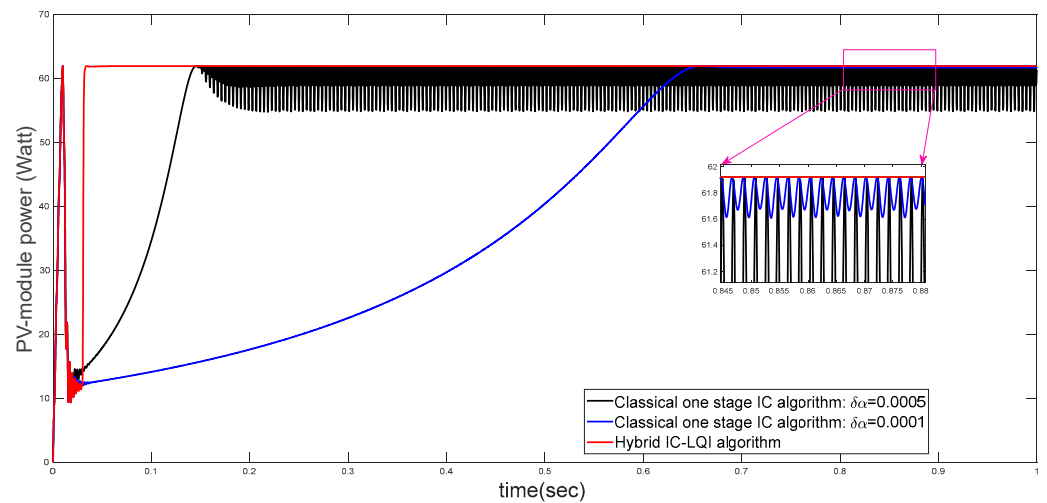


Figure 9. PV-module power using synthesized MPPT controllers in standard weather condition.

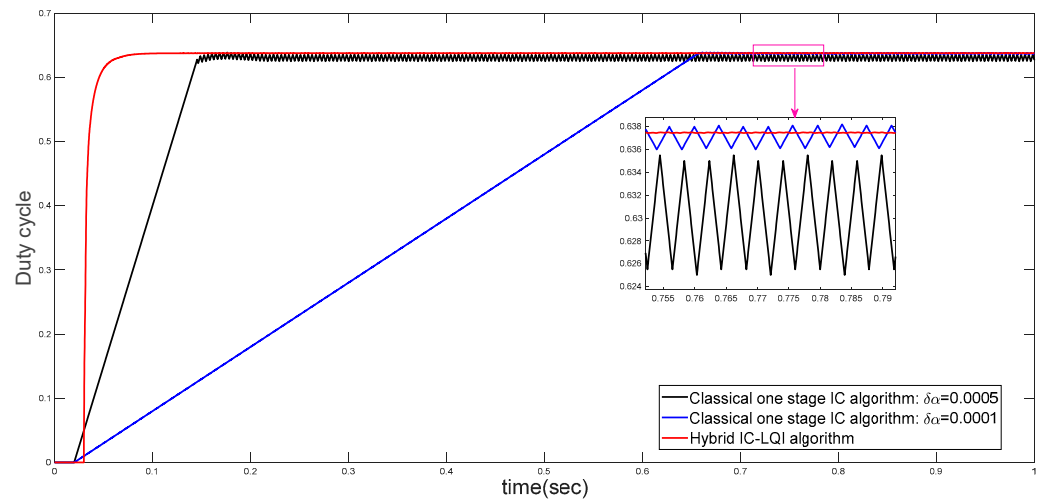


Figure 10. Duty cycle using synthesized MPPT controllers in standard weather condition.

4.2. Second Test Scenario: Simulation under Step Changes of Both Temperature and Irradiance

In real life, temperature and irradiance variations are synchronized. Figure 11 shows the evolution of these factors during the simulation time. In this scenario, the PV-module power and the command signal are shown in Figures 12 and 13 respectively, for the synthesized MPPT techniques. Figure 12 shows that the MPPT controllers follow the variations of the MPP caused by step changes of weather factors. However, the results are significantly different, as the flaws of the classical method of one-stage are visible. By utilizing the hybrid IC-LQI technology, these problems are addressed. This algorithm is better because it exhibits a quicker response and a smoother output power. Figure 13 presents the multiple MPP levels that are guaranteed, since the variations of the duty cycle have the same shape of the output PV-module power. In the same figure, one can see the superiority of the command signal using our proposal compared to the classical IC algorithm.

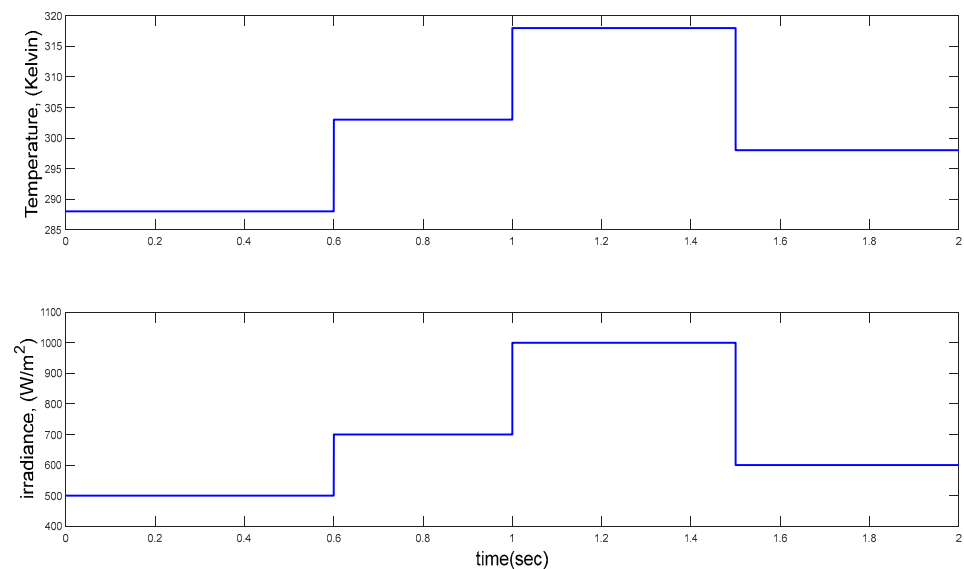


Figure 11. Step change in irradiance and temperature used in the second scenario.

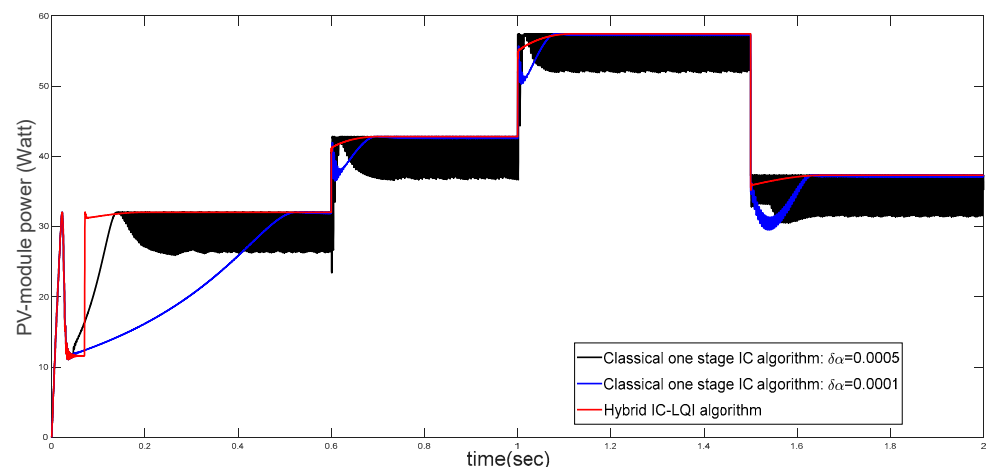


Figure 12. PV-module power using different synthesized MPPT approaches with step changes in both temperature and irradiance.

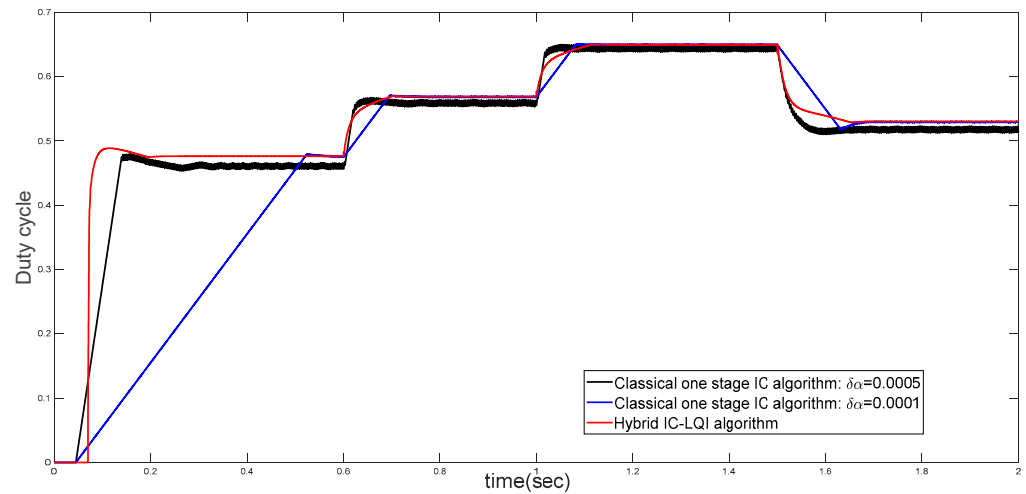


Figure 13. Duty cycle using different synthesized MPPT approaches with step changes in both temperature and irradiance.

4.3. Third Test Scenario: Simulation with Step Changes in Both Weather and Load

The step changes of the load illustrated in Figure 14—which are also typical in the real world—are added to the variations in temperature and irradiance of the second scenario to assess the robustness and efficacy of the proposal. Simulation results of this scenario are presented in Figures 15 and 16. Figure 15 shows that the MPP is guaranteed by using all the MPPT techniques. However, our proposal is superior because it again presents a smoother output power, a faster response and less power drop compared to the other approach. As can be observed from the zoom portions, the simultaneous step changes of the three components have an impact on the classical one-stage IC approach, which exhibits considerable power losses and a long settling time when selecting $\delta\alpha = 10^{-4}$. By choosing $\delta\alpha = 5 \times 10^{-4}$, the response speed is improved where the settling time is lowered, however oscillations are still seen around the MPPs that rely on the load’s value.

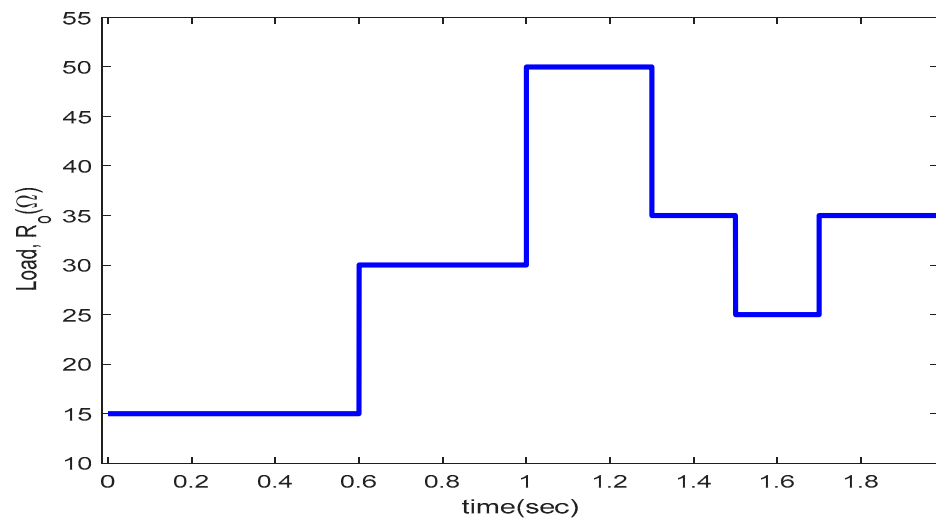


Figure 14. Step-change of the resistive load utilized in the third scenario.

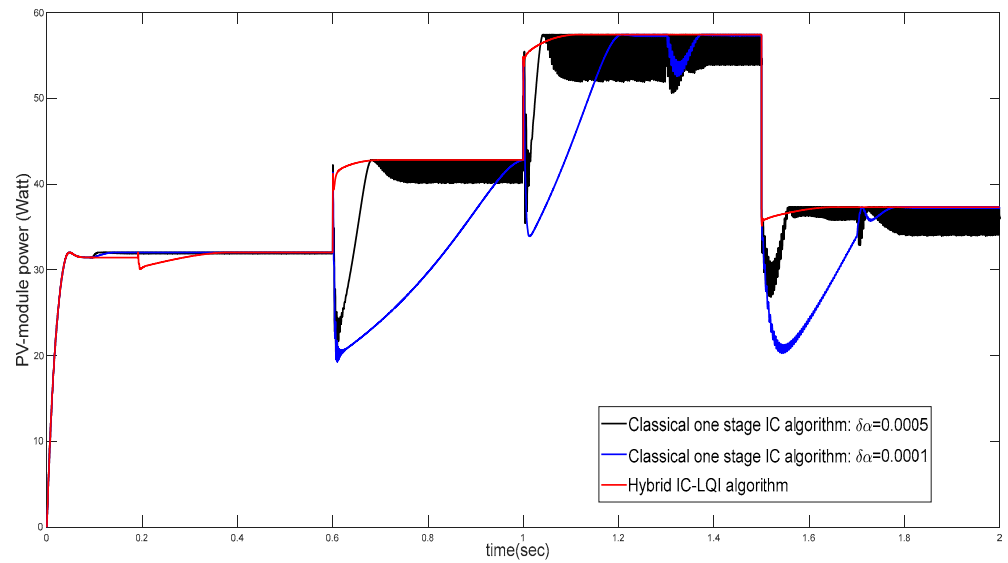


Figure 15. PV-module power using different synthesized MPPT approaches with simultaneous step change of temperature, irradiance and load.

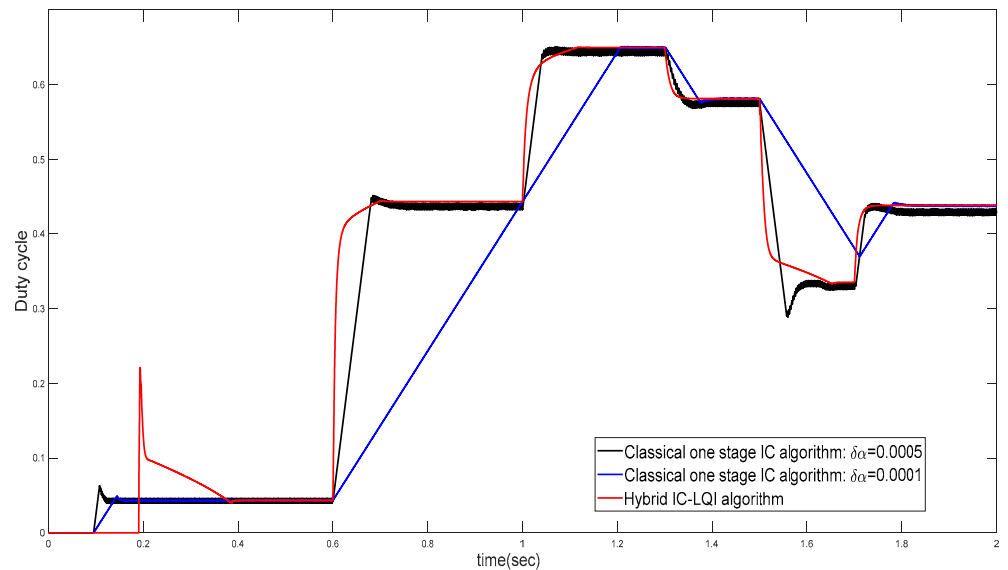


Figure 16. Duty cycle using different synthesized MPPT approaches with simultaneous step change of temperature, irradiance and load.

4.4. Quantitative Comparison Based on Efficiency Criteria

The quality of an MPPT controller can be defined as the ratio between the energy obtained at the operating point of the PV-module (p_{MPPT}) and the energy that would be produced at the MPP (p_{Max}). By integrating the power over a period of time, these energies are produced. η_{MPPT} stands for operating efficiency and is expressed as a percentage (%):

$$\eta_{MPPT} = \frac{\sum_{i=1}^N p_{MPPT}(i)}{\sum_{i=1}^N p_{Max}(i)} \times 100 \tag{28}$$

where N is the number of samples and the simple sum of power samples is used to conduct the power integration at predetermined intervals.

Table 2 and the histogram of Figure 17 show that the hybrid IC-LQI approaches yield better efficiency η_{MPPT} (highlighted in bold) than the one stage IC algorithm.

Table 2. Comparing MPPT controllers on the basis of efficiency.

	Classical One Stage IC Algorithm with $\delta\alpha = 5 \times 10^{-4}$	Classical One Stage IC Algorithm with $\delta\alpha = 1 \times 10^{-4}$	Hybrid IC-LQI Algorithm
Scenario 1	89.4%	65.57%	98.05%
Scenario 2	95.82%	91.3%	98.24%
Scenario 3	96.10%	87.75%	98.92%

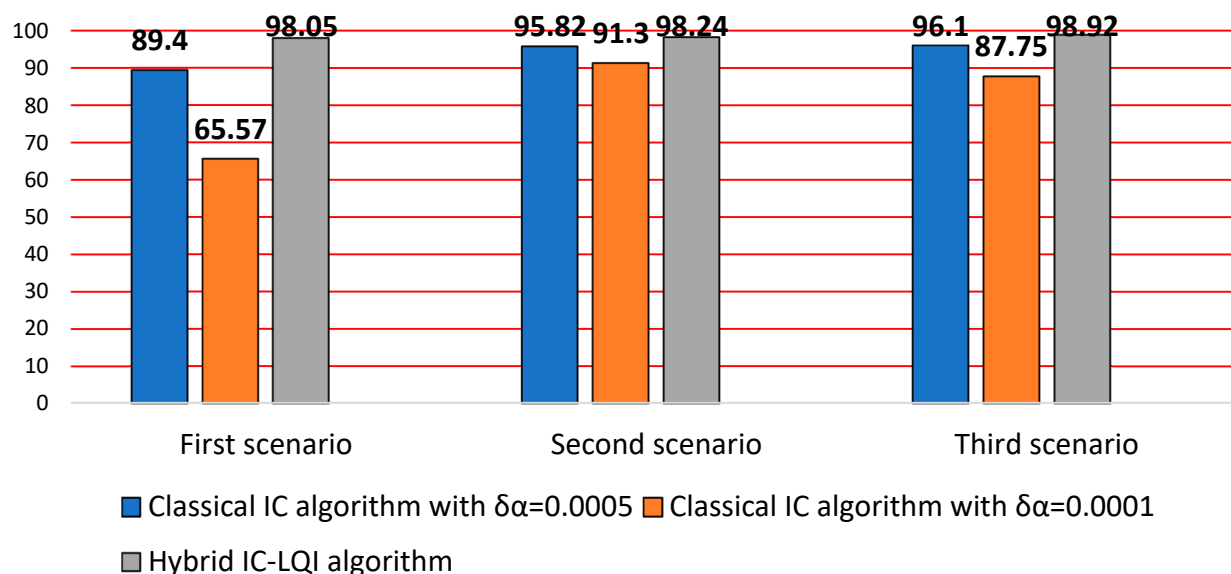


Figure 17. Histogram of simulation scenarios versus efficiency η_{MPPT} .

The difference between the maximum and minimum efficiency in the three scenarios changes very little when using the proposed controller; it is estimated to be just 0.87%. This is in contrast to the classical IC algorithm, where the differences increase, rising to 6.7% using $\delta\alpha = 5 \times 10^{-4}$ and 25.73% using $\delta\alpha = 10^{-4}$.

5. Conclusions

This paper has developed a novel MPPT controller integrated in a standalone PV system. It consists of the hybridization of the Incremental Conductance (IC) technique and the Linear Quadratic Integral (LQI) controller, named IC-LQI technique. Simulated results show that this IC-LQI MPPT technique tracks rapidly the MPP with a significant reduction of oscillations and gives a high efficiency of up to 98.18%. The results obtained under different scenarios reveal that the proposed hybrid IC-LQI technique performs better than the IC technique in terms of efficiency, tracking speed, transient oscillations and steady state performance. The hybrid IC-LQI controller has also shown being capable of tracking the MPP despite sudden changes in irradiation, temperature and load. The proposed IC-LQI controller is also distinguished by its simple implementation in MPPT control. Then, it is concluded that the proposed hybrid IC-LQI is an effective technique to maximize the output PV power of PV systems under different uniform levels of irradiation, temperature and load. Based on these evaluations and remarks, the next stage of this work is to execute the hardware validation of the proposed hybrid IC-LQI MPPT controller.

Author Contributions: Conceptualization, N.B.; methodology, N.B., Y.H., A.D. and V.F.-B.; Software, N.B.; validation, N.B., Y.H., A.D. and V.F.-B.; formal analysis, N.B. and V.F.-B.; investigation, N.B., Y.H., A.D. and V.F.-B.; resources, N.B., A.L. and B.B.; data curation, N.B.; writing—original draft preparation, N.B., Y.H. and A.D.; writing—review and editing, V.F.-B.; visualization, N.B., Y.H., A.D. and V.F.-B.; supervision, V.F.-B.; project administration, N.B., A.L. and B.B.; funding acquisition, V.F.-B. All authors have read and agreed to the published version of the manuscript.

Funding: This work has been financially supported in part by the Directorate-General for Scientific Research and Technological Development-Algerian Ministry of Higher Education and Scientific Research, and in part by the University of Castilla-La Mancha (Spain) and the European Social Fund (FEDER) under Project 2023-GRIN-34307.

Data Availability Statement: The data that support the findings of this study are available from the first author upon reasonable request.

Conflicts of Interest: The authors declare no conflict of interest.

References

- Zahedi, A. Solar photovoltaic (PV) energy; latest developments in the building integrated and hybrid PV systems. *Renew. Energy* **2006**, *31*, 711–718. [\[CrossRef\]](#)
- Salam, Z.; Ahmed, J.; Merugu, B.S. The application of soft computing methods for MPPT of PV system: A technological and status review. *Appl. Energy* **2013**, *107*, 135–148. [\[CrossRef\]](#)
- Li, G.; Jin, Y.; Akram, M.; Chen, X.; Ji, J. Application of bio-inspired algorithms in maximum power point tracking for PV systems under partial shading conditions—A review. *Renew. Sustain. Energy Rev.* **2018**, *81*, 840–873. [\[CrossRef\]](#)
- Ilyas, A.; Ayyub, M.; Khan, M.R.; Husain, M.A.; Jain, A. Hardware implementation of perturb and observe maximum power point tracking algorithm for solar photovoltaic system. *Trans. Electr. Electron. Mater.* **2018**, *19*, 222–229. [\[CrossRef\]](#)
- Safari, A.; Mekhilef, S. Simulation and hardware implementation of incremental conductance MPPT with direct Control method using cuk converter. *IEEE Trans. Ind. Electron.* **2010**, *58*, 1154–1161. [\[CrossRef\]](#)
- Kivimaki, J.; Kolesnik, S.; Sitbon, M.; Suntio, T.; Kuperman, A. Revisited perturbation frequency design guideline for direct fixed-step maximum power point tracking algorithms. *IEEE Trans. Ind. Electron.* **2017**, *64*, 4601–4609. [\[CrossRef\]](#)
- Farhat, M.; Barambones, O.; Sbita, L. A real-time implementation of novel and stable variable step size MPPT. *Energies* **2020**, *13*, 4668. [\[CrossRef\]](#)
- Owusu-Nyarko, I.; Elgenedy, M.A.; Abdelsalam, I.; Ahmed, K.H. Modified variable step-size incremental conductance MPPT technique for photovoltaic systems. *Electronics* **2021**, *10*, 2331. [\[CrossRef\]](#)
- Singh, P.; Shukla, N.; Gaur, P. Modified variable step incremental-conductance MPPT technique for photovoltaic system. *Int. J. Inf. Technol.* **2020**, *13*, 2483–2490. [\[CrossRef\]](#)
- Zhang, X.; Li, S.; He, T.; Yang, B.; Yu, T.; Li, H.; Jiang, L.; Sun, L. Memetic reinforcement learning based maximum power point tracking design for PV systems under partial shading condition. *Energy* **2019**, *174*, 1079–1090. [\[CrossRef\]](#)
- Atia, M.; Ahriche, A.; Bouarroudj, N. Incremental Conductance Algorithm Based On Indirect Control Mode Using An Integrator Controller Tuned by Routh Criterion. In Proceedings of the 2020 6th International Symposium on New and Renewable Energy (SIENR), Ghardaia, Algeria, 13–14 October 2021; pp. 1–5. [\[CrossRef\]](#)
- Bouarroudj, N.; Benlahbib, B.; Houam, Y.; Sedraoui, M.; Batlle, V.F.; Abdelkrim, T.; Boukhetala, D.; Boudjema, F. Fuzzy based incremental conductance algorithm stabilized by an optimal integrator for a photovoltaic system under varying operating conditions. *Energy Sources Part A Recover. Util. Environ. Eff.* **2021**, 1–26. [\[CrossRef\]](#)
- Bouarroudj, N.; Benlahbib, B.; Sedraoui, M.; Feliu-Batlle, V.; Bechouat, M.; Boukhetala, D.; Boudjema, F. A new tuning rule for stabilized integrator controller to enhance the indirect control of incremental conductance MPPT algorithm: Simulation and practical implementation. *Optik* **2022**, *268*, 169728. [\[CrossRef\]](#)
- Chiu, C.-S.; Ouyang, Y.-L.; Ku, C.-Y. Terminal sliding mode control for maximum power point tracking of photovoltaic power generation systems. *Sol. Energy* **2012**, *86*, 2986–2995. [\[CrossRef\]](#)
- Kihal, A.; Krim, F.; Laib, A.; Talbi, B.; Afghoul, H. An improved MPPT scheme employing adaptive integral derivative sliding mode control for photovoltaic systems under fast irradiation changes. *ISA Trans.* **2018**, *87*, 297–306. [\[CrossRef\]](#) [\[PubMed\]](#)
- Oubbati, B.K.; Boutoubat, M.; Rabhi, A.; Belkheiri, M. Experiential integral backstepping sliding mode controller to achieve the maximum power point of a PV system. *Control Eng. Pract.* **2020**, *102*, 104570. [\[CrossRef\]](#)
- Bouarroudj, N.; Boukhetala, D.; Feliu-Batlle, V.; Boudjema, F.; Benlahbib, B.; Batoun, B. Maximum power point tracker based on fuzzy adaptive radial basis function neural network for PV-system. *Energies* **2019**, *12*, 2827. [\[CrossRef\]](#)
- Ishaque, K.; Salam, Z.; Lauss, G. The performance of perturb and observe and incremental conductance maximum power point tracking method under dynamic weather conditions. *Appl. Energy* **2014**, *119*, 228–236. [\[CrossRef\]](#)
- Karamov, D.N.; Suslov, K.V. Structural optimization of autonomous photovoltaic systems with storage battery replacements. *Energy Rep.* **2021**, *7*, 349–358. [\[CrossRef\]](#)

20. Yousri, D.; Thanikanti, S.B.; Allam, D.; Ramachandaramurthy, V.K.; Eteiba, M. Fractional chaotic ensemble particle swarm optimizer for identifying the single, double, and three diode photovoltaic models' parameters. *Energy* **2020**, *195*, 116979. [[CrossRef](#)]
21. Bouarroudj, N.; Abdelkrim, T.; Farhat, M.; Feliu-Batlle, V.; Benlahbib, B.; Boukhetala, D.; Boudjema, F. Fuzzy logic controller based maximum power point tracking and its optimal tuning in photovoltaic systems. *Serbian J. Electr. Eng.* **2021**, *18*, 351–384. [[CrossRef](#)]
22. Nousiainen, L.; Puukko, J.; Mäki, A.; Messo, T.; Huusari, J.; Jokipii, J.; Viinamäki, J.; Lobera, D.T.; Valkealahti, S.; Suntio, T. Photovoltaic generator as an input source for power electronic converters. *IEEE Trans. Power Electron.* **2012**, *28*, 3028–3038. [[CrossRef](#)]
23. Shang, L.; Guo, H.; Zhu, W. An improved MPPT control strategy based on incremental conductance algorithm. *Prot. Control Mod. Power Syst.* **2020**, *5*, 14. [[CrossRef](#)]
24. Saidi, K.; Maamoun, M.; Bounekhla, M. Simulation and implementation of incremental conductance MPPT algorithm with indirect control method using buck converter. In Proceedings of the 2017 6th International Conference on Systems and Control (ICSC), Batna, Algeria, 7–9 May 2017; pp. 199–204. [[CrossRef](#)]
25. Gurung, N.; Bhattarai, R.; Kamalasan, S. Optimal linear-quadratic-integral controller design for doubly-fed induction generator. In Proceedings of the 2017 IEEE Power & Energy Society General Meeting, Chicago, IL, USA, 16–20 July 2017; pp. 1–5. [[CrossRef](#)]
26. Okyere, E.; Bousbaine, A.; Poyi, G.T.; Joseph, A.K.; Andrade, J.M. LQR controller design for quad-rotor helicopters. *J. Eng.* **2019**, *2019*, 4003–4007. [[CrossRef](#)]

Disclaimer/Publisher's Note: The statements, opinions and data contained in all publications are solely those of the individual author(s) and contributor(s) and not of MDPI and/or the editor(s). MDPI and/or the editor(s) disclaim responsibility for any injury to people or property resulting from any ideas, methods, instructions or products referred to in the content.